

# Observation of an excess of di-charmonium events in the four-muon final state with the ATLAS detector

The ATLAS Collaboration



Alina Isobel Hagan  
Lancaster University  
Beauty 2023 - 03/07/23

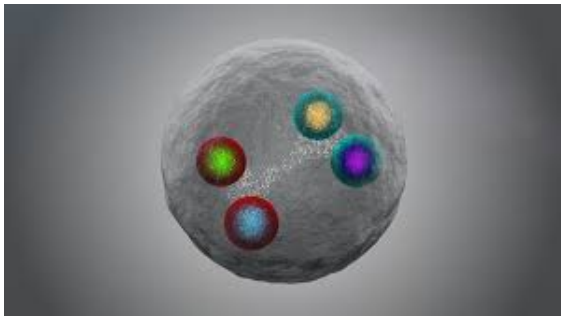
# Introduction

## Introduction

### Contents:

1	Introduction
2	Detector
3	Samples
4	Fits & models
5	Results
6	Systematics
7	Conclusion

- Tetraquark and pentaquark states can exist under color confinement.
- Evidence for a candidate recorded by the Belle Collaboration in 2003, the  $X(3872)$ .



### References:

- Belle - [0309032]
- LHCb - [2006.16957]
- Image: CERN

- New 'particle zoo', evolution of hadron spectroscopy
- LHCb 2020: narrow structure, 6.9GeV, di- $J/\psi(4\mu)$  channel
- Possible to interperate this state,  $X(6900)$ , as a full-charm tetraquark,  $T_{cc\bar{c}\bar{c}}$

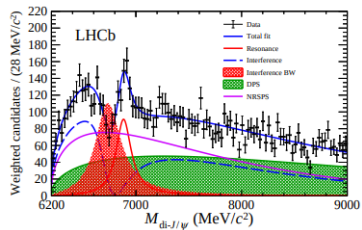
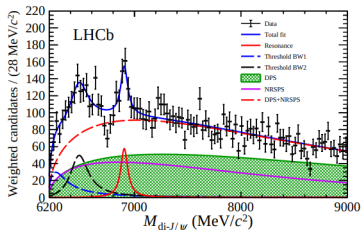
# Introduction

## Introduction

### Contents:

- 1 Introduction
- 2 Detector
- 3 Samples
- 4 Fits & models
- 5 Results
- 6 Systematics
- 7 Conclusion

- LHCb also sees an enhancement in the mass spectrum closer to the di- $J/\psi$  threshold.
- $X(6900)$  is above  $J/\psi+\psi(2S)$  threshold, could observe this in two channels.



- ATLAS explores di- $J/\psi$  and  $J/\psi+\psi(2S)$ , with  $140\text{fb}^{-1}$ ,  $4\mu$  final states.
- Data collected at  $\sqrt{s}=13\text{TeV}$  2015-2018.

### References:

- LHCb - [2006.16957]

# The ATLAS Detector

Detector

## Contents:

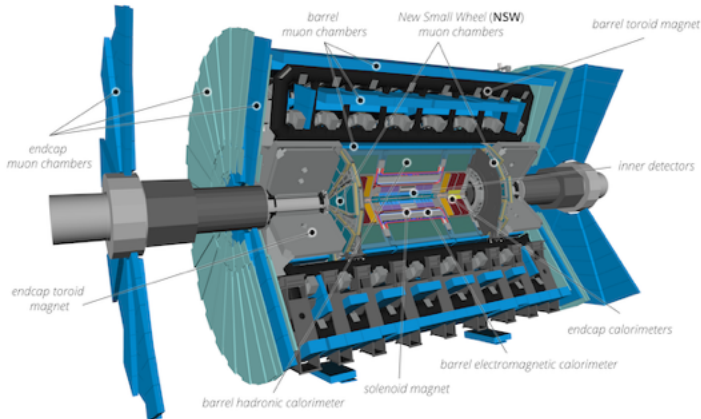
- 1 Introduction
- 2 Detector
- 3 Samples
- 4 Fits & models
- 5 Results
- 6 Systematics
- 7 Conclusion

## References:

- ATLAS - [2305.16623]
- ATLAS Schematic

4/17

- The ATLAS experiment is a general purpose detector with a forward-backwards cylindrical geometrey and nearly complete  $4\pi sr$  coverage in solid angle.
- There are four main components; The inner detector, LAr EM Calorimeter, Hadronic tile calorimeter, Muon spectrometer



- Two stage trigger, L1 and HLT, hardware and software.

# MC Samples

## Samples

### Contents:

1	Introduction
2	Detector
3	<b>Samples</b>
4	Fits & models
5	Results
6	Systematics
7	Conclusion

- Estimation of signal and background contribution; derive from combination of MC and data.
- Multiple background sources;
  - di- $J/\psi$  from SPS and DPS
  - Non-prompt  $J/\psi$  from  $b$
  - Uncorrelated prompt  $J/\psi$  and non-resonant  $\mu\mu$  pairs.
- Single or no  $Q$  background events are modelled using data.
- $J/\psi + \psi(2S)$  feed-down is included in relevant backgrounds.
- MC samples are reweighted for pileup correction.

# Data Sample and selection

Samples

## Contents:

1	Introduction
2	Detector
3	Samples
4	Fits & models
5	Results
6	Systematics
7	Conclusion

- Selection with dimuon and 3-muon trigger, muon pair with mass in  $j/\psi$  or  $\psi(2S)$  range.
- Use the loose criteria for all muon candidates, the thresholds on muon momentum depend on trigger and muon identification requirements.
- Combinations of these triggers with various prescales are used to maximise acceptance, 72% efficiency vs offline.
- $4\mu$  candidate events with two OS pairs; fit all tracks to a vertex.
- Discovered charmonium candidates are refit with a  $J/\psi$  or  $\psi(2S)$ .
- Accept the  $4\mu$  candidate with the lowest  $\chi^2/N$

# Background Modelling

Samples

## Contents:

1	Introduction
2	Detector
3	Samples
4	Fits & models
5	Results
6	Systematics
7	Conclusion

- Reduction of the background by restricting of the  $4\mu$  fit quality ( $\chi^2/N$ ) & limit the transverse distances between the primary vertex and the reconstructed  $4\mu$  vertex and di- $\mu$  sub-vertices.
- Signal and control defined below and above  $\Delta R=0.25$ , respectively.
- Event generator doesn't provide most accurate model of SPS and DPS backgrounds in di- $J/\psi$   $p_T$ ,  $\Delta\phi$ , and  $\Delta\eta$ .
- Make kinematic corrections to this using two control regions.
- Also model the non-prompt background using MC, control regions created by inverting the vertex quality and transverse distance cuts.

Signal region	Control region	Non-prompt region
Di-muon or tri-muon triggers, oppositely charged muons from each charmonium, <i>loose</i> muons, $p_T^{1,2,3,4} > 4, 4, 3, 3$ GeV and $ \eta_{1,2,3,4}  < 2.5$ for the four muons, $m_{J/\psi} \in [2.94, 3.25]$ GeV, or $m_{\psi(2S)} \in [3.56, 3.80]$ GeV, Loose vertex requirements $\chi_{4\mu}^2/N < 40$ ( $N = 5$ ) and $\chi_{\text{di-}\mu}^2/N < 100$ ( $N = 2$ ),		
Vertex $\chi_{4\mu}^2/N < 3$ , $L_{xy}^{4\mu} < 0.2$ mm, $ L_{xy}^{\text{di-}\mu}  < 0.3$ mm, $m_{4\mu} < 11$ GeV,		Vertex $\chi_{4\mu}^2/N > 6$ ,
$\Delta R < 0.25$ between charmonia	$\Delta R \geq 0.25$ between charmonia	or $ L_{xy}^{\text{di-}\mu}  > 0.4$ mm

# Background models, feeddown & selection summary

Samples

## Contents:

1	Introduction
2	Detector
3	Samples
4	Fits & models
5	Results
6	Systematics
7	Conclusion

- Single  $Q$  non-resonant di- $\mu$  events are modelled using data-driven approach as MC also struggles to produce an accurate representation of this background contribution.
- Create CR here by requiring one  $Q$  candidate is reconstructed with a track from something other than a muon candidate.
- For di- $J/\psi$ , feeddown from the  $J/\psi + \psi(2S)$  channel in the form of  $\psi(2S) \rightarrow J/\psi + X$  decays are accounted for;

$$N_{fd} = \frac{B' \epsilon'}{B(\psi(2S) \rightarrow \mu\mu)} N$$

- $\epsilon$  is the efficiency, ( $\epsilon'$  feeddown),  $N$  are the yields, and  $B$  are the branching fractions.
- $B'$  is the branching fraction of the cascading feeddown;

$$B' = [B(\psi(2S) \rightarrow J/\psi + X) + B(\psi(2S) \rightarrow \gamma \chi_{cJ}) B(\chi_{cJ} \rightarrow \gamma J/\psi)] \cdot B(J/\psi \rightarrow \mu\mu)$$



# Signal Extraction

Fits & models

## Contents:

1	Introduction
2	Detector
3	Samples
4	Fits & models
5	Results
6	Systematics
7	Conclusion

- Use an unbinned maximum likelihood fit for the extraction of the signal in the  $4\mu$  mass spectrum with the following likelihood function;

$$\mathcal{L} = \mathcal{L}_{SR}(\vec{\theta}, \vec{\lambda}) \cdot \mathcal{L}_{CR}(\vec{\theta}) \cdot \prod_{j=1}^K G(\theta'_j; \theta_j, \sigma_j)$$

- $\mathcal{L}_{SR, CR}$  are the signal and control region likelihoods.  $\vec{\lambda}$  are the parameters of interest and  $\theta_j$  are the nuisance parameters.
- Background yields in the signal and control regions are constrained together by a transfer factor which is obtained from the aforementioned background modelling.
- Two models are considered for each of the channels under examination.

# Di- $J/\psi$ Models

Fits & models

## Contents:

1	Introduction
2	Detector
3	Samples
4	Fits & models
5	Results
6	Systematics
7	Conclusion

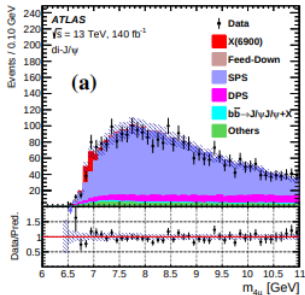
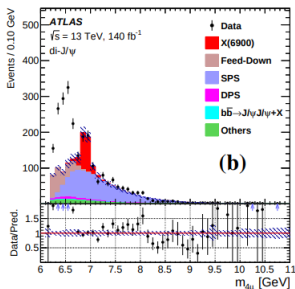
- Model A for the di- $J/\psi$  channel, signal p.d.f. consists of three interfering Breit-Wigners, a phase space factor, and a convolution with a mass resolution function.

$$f_s(x) = \left[ \sum_{i=0}^2 \frac{z_i}{m_i^2 - x^2 - im_i \Gamma_i(x)} \right]^2 \sqrt{1 - \frac{4m_{J/\psi}^2}{x^2}} \otimes R(\theta)$$

- B reduces to two resonances, one non-interfering, and the other interacting with the SPS background, p.d.f.;

$$f(x) = \left[ \frac{z_0}{m_0^2 - x^2 - im_0 \Gamma_0(x)} + A e^{i\phi} \right]^2 + \left[ \frac{z_2}{m_2^2 - x^2 - im_2 \Gamma_2(x)} \right]^2 \sqrt{1 - \frac{4m_{J/\psi}^2}{x^2}} \otimes R(\theta)$$

- $A$ ,  $\phi$  define the SPS background amplitude and phase to  $m_0$ .
- These models are analogous to those in the LHCb study, though interferences between the signal resonances occur in model A, unlike in the LHCb work.



# $J/\psi + \psi(2S)$ Models

Fits & models

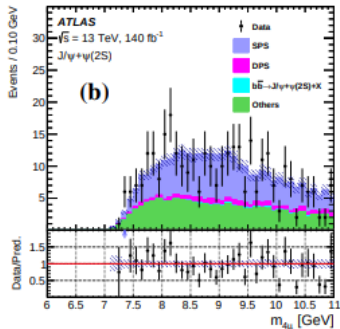
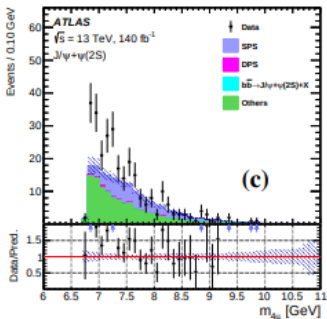
## Contents:

- 1 Introduction
- 2 Detector
- 3 Samples
- 4 Fits & models
- 5 Results
- 6 Systematics
- 7 Conclusion

- For  $J/\psi + \psi(2S)$  channel, model  $\alpha$ , introduce a 4th non-interfering resonance, assuming the resonances also decay to  $J/\psi + \psi(2S)$ ;

$$f_s(x) = \left( \left[ \sum_{i=0}^2 \frac{z_i}{m_i^2 - x^2 - im_i \Gamma_i(x)} \right]^2 + \left[ \frac{z_3}{m_3^2 - x^2 - im_3 \Gamma_3(x)} \right]^2 \right) \cdot \sqrt{1 - \frac{(m_{J/\psi} + m_{\psi(2S)})^2}{x^2}} \otimes R(\theta)$$

- Other model, known as model  $\beta$ , single resonance.



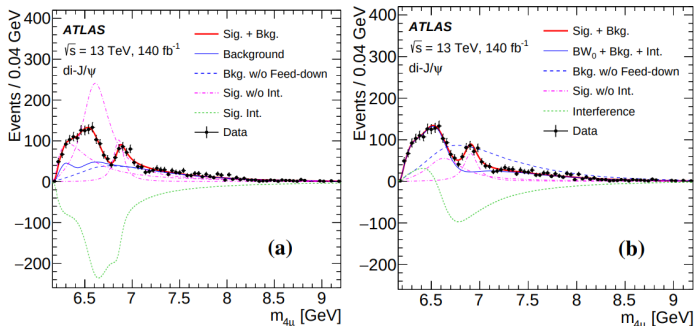
# Di- $J/\psi$ results

Results

## Contents:

- 1 Introduction
- 2 Detector
- 3 Samples
- 4 Fits & models
- 5 Results
- 6 Systematics
- 7 Conclusion

- Models A and B, shown left and right respectively, reproduce the data well.
- A significant excess of events above the background is observed here in the di- $J/\psi$  channel.



- The broad structure at lower mass could result from other effects like feeddown from the higher di- $Q$  resonances, for example  $T_{cc\bar{c}\bar{c}} \rightarrow \chi_{cJ} \chi_{cJ'} \rightarrow J/\psi J/\psi \gamma \gamma$

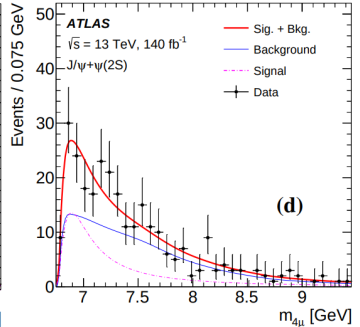
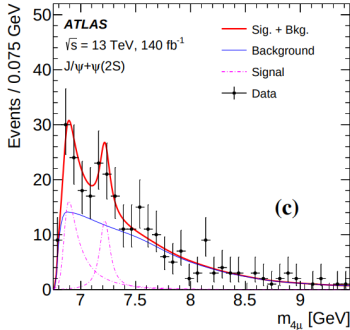
# $J/\psi + \psi(2S)$ results

Results

## Contents:

- 1 Introduction
- 2 Detector
- 3 Samples
- 4 Fits & models
- 5 **Results**
- 6 Systematics
- 7 Conclusion

- The signal significance with signal shape parameters of model  $\alpha$  reaches  $4.7\sigma$ , and  $4.3\sigma$  for model  $\beta$ .



- For model  $\alpha$ , the significance of the second resonance alone is  $3.0\sigma$

# Summary

## Results

### Contents:

1	Introduction
2	Detector
3	Samples
4	Fits & models
5	Results
6	Systematics
7	Conclusion

- The parameters extracted from the fit to the  $m_{4\mu}$  spectrum in both channels is shown below.

di- $J/\psi$	model A	model B
$m_0$	$6.41 \pm 0.08^{+0.08}_{-0.03}$	$6.65 \pm 0.02^{+0.03}_{-0.02}$
$\Gamma_0$	$0.59 \pm 0.35^{+0.12}_{-0.20}$	$0.44 \pm 0.05^{+0.06}_{-0.05}$
$m_1$	$6.63 \pm 0.05^{+0.08}_{-0.01}$	—
$\Gamma_1$	$0.35 \pm 0.11^{+0.11}_{-0.04}$	—
$m_2$	$6.86 \pm 0.03^{+0.01}_{-0.02}$	$6.91 \pm 0.01 \pm 0.01$
$\Gamma_2$	$0.11 \pm 0.05^{+0.02}_{-0.01}$	$0.15 \pm 0.03 \pm 0.01$
$\Delta s/s$	$\pm 5.1\%^{+8.1\%}_{-8.9\%}$	—
$J/\psi+\psi(2S)$	model $\alpha$	model $\beta$
$m_3$ or $m$	$7.22 \pm 0.03^{+0.01}_{-0.03}$	$6.96 \pm 0.05 \pm 0.03$
$\Gamma_3$ or $\Gamma$	$0.09 \pm 0.06^{+0.06}_{-0.03}$	$0.51 \pm 0.17^{+0.11}_{-0.10}$
$\Delta s/s$	$\pm 21\% \pm 14\%$	$\pm 20\% \pm 12\%$

- The significance for all resonances and for the  $X(6900)$  exceeds  $5\sigma$ ,  $m_2$  aligns with the LHCb mass.
- As is with the LHCb paper, a broad structure at lower mass and a resonance around 6.9GeV are seen.

# Systematics

## Systematics

### Contents:

1	Introduction
2	Detector
3	Samples
4	Fits & models
5	Results
6	Systematics
7	Conclusion

- Systematics uncertainties are considered to be only those producing an effect on the normalisations and the mass lineshape, though only perturbations of the lineshape are of concern, signal and background normalisations are free-floating parameters.

Systematic Uncertainties (MeV)	di- $J/\psi$		$J/\psi+\psi(2S)$	
	$m_2$	$\Gamma_2$	$m_3$	$\Gamma_3$
Muon calibration	$\pm 6$	$\pm 7$	$< 1$	$\pm 1$
SPS model parameter	$\pm 7$	$\pm 7$	$< 1$	
SPS di-charmonium $p_T$	$\pm 7$	$\pm 8$	$< 1$	
Background MC sample size	$\pm 7$	$\pm 8$	$\pm 1$	$< 1$
Mass resolution	$\pm 4$	$-3$	$-1$	$^{+2}_{-4}$
Fit bias	$-13$	$+10$	$^{+9}_{-10}$	$^{+50}_{-16}$
Shape inconsistency	$< 1$		$\pm 4$	$\pm 6$
Transfer factor	—		$\pm 5$	$\pm 23$
Presence of 4th resonance	$< 1$		—	
Feed-down	$^{+4}_{-1}$	$^{+6}_{-2}$	—	—
Interference of 4th resonance	—		$-32$	$-11$
P and D-wave BW	$+9$	$+19$	$< 1$	$\pm 1$
$\Delta R$ and muon $p_T$ requirements	$^{+3}_{-2}$	$^{+6}_{-4}$	$^{+1}_{-2}$	$-2$

- Systematic uncertainties in  $m_{4\mu}$  are treated as resolution effects, which are dependent on the mass range.

# Conclusion

## Conclusion

### Contents:

1	Introduction
2	Detector
3	Samples
4	Fits & models
5	Results
6	Systematics
7	Conclusion

- Summary; search of a possible  $cc\bar{c}\bar{c}$  state decaying into a  $Q$  pair, either two  $J/\psi$  or a  $J/\psi$  and  $\psi(2S)$  in  $4\mu$  state, with  $\sqrt{s}=13\text{TeV}$  at the ATLAS detector.
- With  $140\text{fb}^{-1}$  a large excess, of significance over  $5\sigma$ , is seen in the  $di\text{-}J/\psi$  channel
- Broad structure at low mass is seen along with the resonance at  $6.9\text{GeV}$ .
- A three-resonance model with interferences and a model with the broader structure at lower  $m_{4\mu}$  are more successful in describing the lineshape than cases with less or no interference.
- For the  $J/\psi+\psi(2S)$  channel the excess is of the order  $4.7\sigma$  when using a two-resonance model, one of which is near the  $6.9\text{GeV}$  threshold.
- The lower-mass structure cannot be discerned in detail with current data, interpretations including non-interfering resonances, reflections and threshold enhancements cannot be discounted.



# Conclusion

## Conclusion

### Contents:

1	Introduction
2	Detector
3	Samples
4	Fits & models
5	Results
6	Systematics
7	Conclusion

- Summary; search of a possible  $cc\bar{c}\bar{c}$  state decaying into a  $Q$  pair, either two  $J/\psi$  or a  $J/\psi$  and  $\psi(2S)$  in  $4\mu$  state, with  $\sqrt{s}=13\text{TeV}$  at the ATLAS detector.
- With  $140\text{fb}^{-1}$  a large excess, of significance over  $5\sigma$ , is seen in the di- $J/\psi$  channel
- Broad structure at low mass is seen along with the resonance at  $6.9\text{GeV}$ .
- A three-resonance model with interferences and a model with the broader structure at lower  $m_{4\mu}$  are more successful in describing the lineshape than cases with less or no interference.
- For the  $J/\psi+\psi(2S)$  channel the excess is of the order  $4.7\sigma$  when using a two-resonance model, one of which is near the  $6.9\text{GeV}$  threshold.
- The lower-mass structure cannot be discerned in detail with current data, interpretations including non-interfering resonances, reflections and threshold enhancements cannot be discounted.

**Thanks for listening.**